Published in final edited form as:
Macromol Biosci. 2012 August ; 12(8): 1077–1089. doi:10.1002/mabi.201100501.

Enzymatic mineralization of hydrogels for bone tissue engineering by incorporation of alkaline phosphatase

Dr. Timothy E.L. Douglas,
Department of Biomaterials, Radboud University Medical Center Nijmegen, P.O. Box 9101 6500 HB Nijmegen, the Netherlands. Polymer Chemistry and Biomaterials (PBM) Group, Department of Organic Chemistry, Krijgslaan 281 S4, Ghent University, 9000 Gent, Belgium

Prof. Philip B. Messersmith,
Department of Biomedical Engineering, Chemistry of Life Processes Institute, and Institute for Bionanotechnology in Medicine, Northwestern University, Evanston, IL 60208, USA

Safak Chasan,
Department of Molecular Biology and Genetics, Middle East Technical University, 06531 Ankara, Turkey

Prof. Antonios G. Mikos,
Rice University, Department of Bioengineering, Houston, Texas, USA

Eric L.W. de Mulder,
Department of Orthopedics, Radboud University Medical Center Nijmegen, The Netherlands

Dr. Glenn Dickson,
Centre for Cancer Research and Cell Biology, Queen's University Belfast, 97 Lisburn Road, Belfast BT9 7BL, N. Ireland, UK

David Schaubroeck,
Center for Microsystems Technology (CMST), ELIS, Imec, Technologiepark 914a, 9052 Gent, Belgium

Dr. Lieve Balcaen,
Ghent University, Department of Analytical Chemistry, Krijgslaan 281 - S12, 9000 Ghent, Belgium

Prof. Frank Vanhaecke,
Ghent University, Department of Analytical Chemistry, Krijgslaan 281 - S12, 9000 Ghent, Belgium

Prof. Peter Dubruel,
Polymer Chemistry and Biomaterials (PBM) Group, Department of Organic Chemistry, Krijgslaan 281 S4, Ghent University, 9000 Gent, Belgium

Prof. John A. Jansen, and
Department of Biomaterials, Radboud University Medical Center Nijmegen, P.O. Box 9101 6500 HB Nijmegen, the Netherlands

Dr. Sander C.G. Leeuwenburgh
Department of Biomaterials, Radboud University Medical Center Nijmegen, P.O. Box 9101 6500 HB Nijmegen, the Netherlands

Timothy E.L. Douglas: Timothy.Douglas@UGent.be; Philip B. Messersmith: philm@northwestern.edu; Safak Chasan: e158962@metu.edu.tr; Antonios G. Mikos: mikos@rice.edu; Eric L.W. de Mulder: E.deMulder@orthop.umcn.nl; Glenn

Correspondence to: Sander C.G. Leeuwenburgh, S.Leeuwenburgh@dent.umcn.nl.

T.E.L. Douglas mainly contributed to this manuscript at Radboud University Medical Center Nijmegen (previous affiliation). A further contribution was made at Ghent University (current affiliation).

Dickson: G.Dickson@qub.ac.uk; David Schaubroeck: David.Schaubroeck@elis.ugent.be; Lieve Balcaen: Lieve.Balcaen@UGent.be; Frank Vanhaecke: Frank.Vanhaecke@UGent.be; Peter Dubruel: Peter.Dubruel@UGent.be; John A. Jansen: J.Jansen@dent.umcn.nl; Sander C.G. Leeuwenburgh: S.Leeuwenburgh@dent.umcn.nl

Abstract

Alkaline Phosphatase (ALP), an enzyme involved in mineralization of bone, was incorporated into three hydrogel biomaterials to induce their mineralization with calcium phosphate (CaP). These were collagen type I, a mussel protein-inspired adhesive consisting of PEG substituted with catechol groups, cPEG, and the PEG-fumaric acid copolymer OPF. After incubation in calcium glycerophosphate (Ca-GP) solution, FTIR, EDS, SEM, XRD, SAED, ICP-OES and von Kossa staining confirmed CaP formation. The amount of mineral formed decreased in the order cPEG > collagen > OPF. Mineral:polymer ratio decreased in the order collagen > cPEG > OPF. Mineralization increased Young's modulus, most profoundly for cPEG. Such enzymatically mineralized hydrogel-CaP composites could find application as bone regeneration materials.

Keywords

enzymes; biomineralization; hydrogels; biomaterials; composites

Introduction

Hydrogels are an important class of highly hydrated polymers under increasing investigation for potential uses in tissue engineering. Advantages of hydrogels include injectability and exact fitting to defect sites as well as ease of incorporation of cells and bioactive substances such as growth factors or enzymes. Generally, however, hydrogels lack the ability to mineralize with calcium phosphate (CaP) and form strong interactions with hard tissues such as bone. The most popular mineralization strategy has been the incorporation of inorganic phases such as calcium phosphate ceramics into hydrogel matrices. These inorganic particles act as nucleation sites that enable further mineralization. However CaP particles tend to aggregate, although dispersion can be improved by direct formation of CaP in the hydrogel [1] and use of dispersants such as citrate. [2]

A recent trend in tissue engineering involves the development of hydrogels that possess the capacity to mineralize. Mineralization is anticipated to lead to a number of advantages from both clinical and basic science points of view. Firstly, the presence of CaP mineral can increase the biological performance of bone-substituting materials by the so-called phenomenon of bioactivity, whereby a chemical bond with surrounding bone tissue is formed after implantation. [3] Secondly, another advantage of mineralizing hydrogels lies in the fact that CaP ceramics have an intrinsic affinity for biologically active proteins such as growth factors, which stimulate the natural healing processes of the surrounding bone tissue. [4] Thirdly, mechanical reinforcment due to mineralization may help to overcome one of the main disadvantages of hydrogel materials, namely weak mechanical properties. Fourthly, since stiffer [5, 6] and rougher [7] surfaces are known to promote differentiation of cells towards the osteoblastic phenotype, mineralization is expected to make hydrogels more compatible with bone tissue.

Alkaline Phosphatase (ALP) is an enzyme involved in mineralization of bone by cleavage of phosphate from organic phosphate. [8] The use of ALP to induce homogenous mineralization of hydrogels to increase their mechanical strength or render them more suitable for bone replacement applications is an alternative to incorporation of CaP particles. With the aim of conducting fundamental research into bone cell behavior and principles of biomineralization, ALP was successfully used to mineralize polyHEMA hydrogels [9–11] and artificial self-assembling peptide amphiphile hydrogels. [12] ALP has also been

covalently linked to dentine-derived collagen sheets to induce their mineralization in vivo and in vitro by Beertsen and van den Bos [13–15] and in vitro by Doi et al. [16]

In this study, ALP was incorporated into three hydrogels of interest for bone tissue engineering applications, namely catechol-polyethylene glycol (cPEG), collagen type I and oligo(poly(ethylene glycol) fumarate) (OPF). cPEG is a mussel adhesive protein-inspired adhesive hydrogel consisting of 4-armed polyethylene glycol (PEG) substituted with catechol end-groups, which has shown good biocompatibility in vivo [17] as well as good in vitro cytocompatibility. [18] Collagen type I has been widely used as a hydrogel material for cell encapsulation due to its biocompatibility and similarity to native extracellular matrix (ECM). [19] Oligo(poly(ethylene glycol) fumarate) (OPF), a copolymer of PEG and fumaric acid, was developed as a biodegradable injectable hydrogel cell carrier for orthopedic tissue engineering and has demonstrated cytocompatibility [20] in vitro and biocompatibility in vivo. [21] By inducing enzymatic mineralization of three different hydrogel materials (one natural (collagen) and two synthetic (cPEG, OPF)), it was intended to show the applicability of this approach to a wide range of hydrogels. A further goal of this study was to compare the mineral-forming capacity of the hydrogels as a function of their chemical structural differences. A strategy to increase hydrogel mineralizability is functionalization with calcium-binding groups. [22–24] It was hypothesized that the three hydrogels in this study would differ in mineralization behavior due to the presence of calcium-binding groups. cPEG and OPF were compared as PEG derivatives, a structural difference being the presence of catechol groups in cPEG. Since catechol groups have a high affinity to hydroxyapatite surfaces [25] and have stimulated CaP formation as components of coatings [26], it was predicted that cPEG would show higher mineralization than OPF. Collagen type I, being the main organic ECM component of mineralized bone, was expected to have a high mineralization due to the intrinsic presence of acidic amino acid residues that can bind calcium.

ALP was added before gel formation on the assumption that it would, to some extent, be entrapped in the crosslinked polymer network. This strategy of ALP entrapment during gelation is universally applicable to all hydrogels and avoids the use of potentially toxic crosslinking agents that may also alter enzyme activity during chemical immobilization of the enzyme to the gel. After ALP incorporation, gels were incubated in a calcium glycerophosphate (Ca-GP) solution. Ca-GP diffused into the membrane, where under the action of ALP, phosphate was released which reacted with calcium ions to form calcium phosphate (CaP). The principle is illustrated schematically in Figure 1.

The study aimed to incorporate ALP into the abovementioned hydrogel biomaterials and investigate a) the retention of ALP in the hydrogel and induction of its mineralization; b) the nature and amount of the mineral thus formed and c) the effect of mineralization on hydrogel morphology and mechanical properties.

Experimental Section

Preparation of hydrogels:cPEG

4-arm cPEG was prepared as described previously. [27] 200 mg ml^{-1} cPEG in double-concentrated phosphate buffered saline (PBS), ALP in double-concentrated PBS and 0.08 M $NaIO_4$ (crosslinker) in H_2O were mixed in the volumetric ratio 1:1:2 to yield a gel with a final concentration of 1 x PBS, 50 mg ml^{-1} cPEG and 0, 1.25 or 2.5 mg ml^{-1} ALP. ALP from bovine intestinal mucosa was obtained from Sigma-Aldrich (P7640).

Preparation of hydrogels:OPF

PEG, ammonium persulfate (APS), N,N,N′,N′-tetramethylethylenediamine (TEMED) and triethyl amine were purchased from Aldrich, Milwaukee, WI, USA. Fumaril chloride was obtained from ACROS (Pittsburgh, PA, USA) and was distilled before use. PEG-DA (Nominal molecular weight 4000; Monomer-Polymer & Dajac Labs, Feasterville, USA) was used as crosslinker.

OPF was synthesized from PEG of average molecular weight of 10000 g mol^{-1} (designated 10K OPF) and from Fumaryl Chloride with procedures previously established. [28]

For the preparation of the OPF gels containing ALP, 0.3 g of OPF macromers and 0.15 g PEG-DA cross-linker were added to 1531 μl of phosphate buffered saline (PBS) and left at 37 °C for 15 minutes with shaking in order for the macromers to completely dissolve. Equal volumes of thermal initiators (140.4 μl) 25 mM APS and TEMED were added, as well as 200 μl ALP solution in Milli-Q at concentrations of 0, 12.5 and 25 mg ml^{-1} water. This yielded final ALP concentrations of 0, 1.25 and 2.5 mg ml^{-1} gel. After gentle but rapid mixing, the gels were poured into cylindrical moulds and then left at 37 °C for 15 minutes in order to obtain OPF hydrogels.

Preparation of hydrogels:collagen

Collagen gels of volume 0.5 ml were prepared as described previously. [29] Briefly, 0.4 ml of acidic type I rat tail collagen (BD Biosciences, 354231) at a concentration of 3.74 mg ml^{-1} was added to 0.05 ml of 10x minimum essential medium Eagle (MEM) (Sigma-Aldrich, M0275) and 0.05 ml ALP solution in Milli-Q at concentrations of 0, 12.5 and 25 mg ml^{-1} water. This yielded final ALP concentrations of 0, 1.25 and 2.5 mg ml^{-1} gel. After drop-wise neutralization with 1 M sodium hydroxide, gel formation took place at 37 °C in a water bath. The final concentration of the collagen gel was approximately 3 mg collagen ml^{-1} gel.

Release of active ALP from hydrogels

ALP-loaded gels containing 2.5 mg ALP ml^{-1} gel were incubated in 3 ml ultrapure water. Concentrations of active ALP in the surrounding water were measured 90, 180, 270 and 360 minutes after the start of incubation (n=4) Concentration of active ALP was determined using a standard ALP activity assay [30] with modifications. In brief, 100 μl of incubation medium containing released ALP was transferred to a well of a 96-well plate. 50 μl of a substrate solution consisting of 5 mM p-nitrophenylphosphate disodium salt (Sigma-Aldrich, NL, P5994) in 0.5 M alkaline buffer was added. This buffer was prepared by diluting 1.5 M Alkaline Buffer (Sigma-Aldrich, NL, A9226) with Milli-Q in the volumetric ratio 1:2. After approximately 3 minutes' incubation, the reaction was stopped by addition of 100 μl 0.3 M NaOH (aq). Absorbance was measured at 405 nm. A calibration curve of ALP in water with concentrations ranging from 0 to 0.25 mg ml^{-1} served as a reference.

Mineralization of hydrogels

Resulting gels were mineralized by incubation in 0.1 M calcium glycerophosphate (CaGP) in H_2O for 6 days with daily medium change. After conclusion of mineralization, gels were rinsed three times with ultrapure water and incubated for 1 day in ultrapure water with the aim of removing residual CaGP.

Fourier-Transform Infrared Spectroscopy (FTIR)

The chemical nature of the mineral formed in hydrogels was examined by FTIR analysis using a Perkin Elmer apparatus in reflectance mode. Samples were freeze-dried for 48 h prior to examination. Hydroxyapatite (Merck, Germany) was used as a reference material.

Scanning electron microscopy (SEM) and energy dispersive spectroscopy (EDS)

SEM analysis was performed on a JEOL JSM-5600 instrument. The instrument was used in the secondary electron mode (SEI). The SEM instrument is equipped with an electron microprobe JED 2300 and an EDS detector for elemental analysis. Prior to analysis, all samples were freeze-dried for 48 h followed by coating with a thin conductive layer. In the case of SEM-EDS analysis, samples were coated with a thin carbon layer (ca 15 nm) by flash evaporation. In case of SEM examination, samples were coated with a thin gold layer (ca 20 nm) using a plasma magnetron sputter coater, with the exception of images showing cross-sections, which were taken after carbon coating by flash evaporation.

Detection of Ca and P by inductively coupled plasma optical emission spectroscopy (ICP-OES)

Since ICP-OES is a more reliable method to measure the elemental composition of mineral produced, the concentrations of Ca and P and the Ca/P molar ratio were determined by ICP-OES using a Spectro Arcos Optical Emission Spectrometer (Spectro, Germany). Before analysis, freeze-dried hydrogel samples were dissolved in 2 ml 14 M HNO_3, and further diluted (250×) with 0.3 M HNO_3 (HNO_3 of analytical grade - ChemLab, Belgium). The instrument was calibrated by means of 6 standard solutions with Ca and P concentrations ranging from 0 to 5 mg l^{-1}. Yttrium was added to all solutions as an internal standard in order to correct for possible instrument instabilities and matrix effects.

X-ray diffraction (XRD) and selected area electron diffraction (SEAD)

The crystallographic structure of the mineral formed was characterized by XRD and SAED. For XRD, freeze-dried mineralized cPEG and OPF samples were pressed into thin films. Mineralized collagen was already in powder form after freeze-drying due to the lower solid content and cohesion of collagen gels. XRD measurements were performed using a thin-film X-ray diffractometer with CuKα-radiation (PW 3710, 50 kV, 40 mA) by fixing the sample to a position of 2.5° and scaaning the detector between 20 °2θ and 40 °θ with a step-size of 0.01 °2θ and a counting time of 5 s step $^{-1}$.

For SAED, freeze-dried mineralized cPEG and OPF samples were chopped up with a razor blade to obtain powders. Mineralized collagen was already in powder form after freeze-drying. Powders were crushed between glass slides and then placed into a small volume of acetone, which was subsequently ultrasonicated to break up any remaining aggregates and to create a suspension. A drop of the suspension was placed on a formvar/carbon coated grid and allowed to air dry. The grids were then viewed in a JEOL 100CX II Transmission Electron Microscope at 80 kV. Particles were selected, image focused at a magnification of 40000, camera length set to 100com and the diffraction pattern recorded onto Kodak 4489 Electron Microscope film.

Histological preparation and staining and light microscopy examination

Mineral distribution within hydrogels was visualised by embedding in paraffin and histological sectioning followed by von Kossa staining for calcium phosphate deposits according to standard protocols. Light micrographic images were recorded on a Leica DMLB light microscope fitted with a Leica DC 300 digital image camera and images captured using Leica IM50 image manager software.

Quantification of dry mass percentage after mineralization and mineral:polymer ratio

The dry mass percentage, i.e. the gel weight percentage not consisting of water, was calculated as: (weight after freeze-drying/weight before freeze-drying)*100. This serves as a measure of amount of mineral formed. The mineral:polymer ratio in mineralized hydrogels, which serves as a measure of polymer mineral-forming capacity, was calculated as ((dry mass % - dry mass % at 0 mg ml^{-1} ALP)/dry mass % at 0 mg ml^{-1} ALP)*100, assuming no loss of polymer. For all hydrogels, n=3. Significant differences were calculated using a two-tailed student's t-test with values of $p < 0.05$ considered significant.

Mechanical testing

Gels were subjected to compressive stresses using a Bose ElectroForce BioDynamic bioreactor (BOSE, MN, USA). Gels were placed between piston heads at predefined distance. Displacement was applied at a rate of 2 mm min^{-1} until samples were compressed to 50% of their original height or failure was reached. During displacement force was recorded with a 22 N load cell for every 0.5 seconds using WinTest software (BOSE). Compressive stress was calculated as force recorded divided by cross-sectional area. Compressive strain was calculated as distance moved during compression divided by initial distance between piston heads. Finally, compressive modulus was calculated as the gradient of the curve of stress (y-axis) against strain (x-axis).

In addition, viscoelastic properties of all types of gels were determined using a rheometer (Anton Paar Physica, MCR 301) equipped with a PP25 rotating head of diameter 25 mm. Storage modulus (G') and loss modulus (G'') values were recorded at a frequency of 1.6 Hz. For all hydrogels, n=3. Significant differences were calculated using a two-tailed student's t-test with values of $p < 0.05$ considered significant.

Results and Discussion

Release of active ALP from hydrogels

Release profiles of active ALP from unmineralized gels in water are shown in Figure 2. The percentage cumulative release of active ALP from cPEG was less than 0.1% of the total amount and did not increase from 90 to 360 minutes' incubation, assuming that activity of released ALP was not decreased by the action of the crosslinkers used to induce cPEG and OPF gel formation. In contrast, approximately 17% of active ALP was released from collagen gels within 90 minutes, with an increase to approximately 30% after 360 minutes. OPF has been used as a drug delivery vehicle for the growth factors TGF-β1 and IGF-1, which showed a slow release pattern (approx. 50% TGF-β1 was released from OPF after 3 days). [31] As ALP's molecular weight has been reported to be 185 kD [32] and thus it is a larger molecule than growth factors such as TGF-β1 (25 kD) [33] it is unsurprising that ALP release is hindered to a greater extent. Presumably the pore sizes in cPEG and OPF hydrogels are too small to allow diffusion of ALP. In contrast, approximately 30% of ALP was released from collagen in 6 hours. This higher release is probably a result of the larger pore size of collagen hydrogels due to the lower solid content in collagen gels (3 mg ml^{-1}) compared to the solid contents of 50 mg ml^{-1} and 200 mg ml^{-1} for cPEG and OPF, respectively, and the fact that collagen monomers assemble into fibrils, as evidenced by SEM (Figure 7c) in contrast to cPEG and OPF.

Physicochemical characterization: FTIR, XRD, SAED, EDS, ICP-OES, SEM

FTIR spectra of gels with and without ALP mineralized for 6 days are shown in Figure 3. The spectra of cPEG and collagen changed dramatically; samples containing ALP displayed spectra in which the intensity of peaks characteristic for the polymer was reduced considerably. The spectrum of pure HAP reveals two regions with spectral features. The

spectral features between 900 and 1 200 cm^{-1} arise primarily from the symmetric (v_1) and asymmetric (v_3) P-O stretching modes of the phosphate groups in HAP. [34] Bands in the 500–700 cm^{-1} region arise primarily from the asymmetric P-O bending modes of the phosphate groups. In the case of cPEG, bands typical for PEG were observed such as the C-H stretch at approximately 2 900 cm^{-1} and [the] asymmetric C-O-C stretch at approximately 1 100 cm^{-1}. [35] These bands were no longer evident in the spectra of samples containing ALP. In the case of collagen, typical bands such as the two amide bands (amide I and amide II) in the region 1 700 to 1 500 cm^{-1} corresponding to overlapping signals of C=O stretching, N–H bending and C–N stretching [36, 37] were present in samples without ALP but much less pronounced in samples with ALP. In the case of OPF, characteristic peaks for the polymer are the peaks attributed to PEG (see above) and the band at 1 725 cm^{-1} from the C=O stretch of the ester carbonyl in fumaric units. [28] After ALP mineralization, these bands remained almost completely in the spectrum, suggesting a lower mineral:polymer ratio.

Hence, FTIR provided evidence of CaP formation in collagen and cPEG gels. Yamauchi et al. reported that ALP-induced formation of amorphous CaP and some hydroxyapatite in collagen sheets [38] while other authors reported that ALP incorporation caused predominantly hydroxyapatite formation in polyHEMA gels [9, 10] and artificial peptide amphiphile gels. [12] These studies used lower ALP, calcium and glycerophosphate concentrations and it may be speculated that these concentrations influence the type of mineral formed, which may also be dependent on the type of hydrogel.

XRD diffractograms of mineralized hydrogels are shown in Figure 4. Mineralized cPEG samples displayed main reflection peaks 25.8° (002), 32.0° (211 and 112) and 34.1° (202) which correspond to synthetic hydroxyapatite. [39] Further peaks were seen at 20.8° and 38.5°. Mineralized collagen showed much broader diffraction maxima characteristic for apatite at 26.0° and 31.8°, corresponding to a poorly crystalline apatitic mineral phase consisting of smaller apatite crystals. No diffractogram could be obtained for mineralized OPF.

SAED diffractograms of mineralized hydrogels are shown in Figure 5. Mineralized cPEG and OPF samples displayed patterns corresponding to (002), (211) and (004) planes that are characteristic of rings are characteristic of a crystalline apatite phase. [26, 40, 41] Mineralized collagen samples displayed broader, diffusive rings that correspond to lower crystallite sizes as well as several distinct diffraction spots.

EDS spectra of mineralized hydrogels are shown in Figure 6. All three hydrogel samples containing ALP (Figure 6b, d, f) displayed pronounced Ca and P peaks, which were almost completely absent in cPEG and collagen samples without ALP (Figure 6a, c) and considerably lower in OPF samples without ALP (Figure 6e) providing evidence of CaP formation. OPF samples (Figure 6e, f) also showed minor Na and Cl peaks. NaCl is a component of the PBS used in the creation of OPF gels. This may suggest difficulty in washing NaCl and Ca-GP out of OPF samples. cPEG gels without ALP also displayed minor Na and Cl peaks (Figure 6a), potentially originating from the PBS used during gel formation. On the basis of EDS measurements, the following atomic Ca:P ratios in mineralized samples were determined: cPEG; 1.22; collagen: 1.22; OPF: 1.13.

The mass percentage attributable to Ca and P and the molar Ca:P ratio determined by ICP-OES are given in Table 1. For samples containing ALP, the mass percentages attributable to Ca and P decreased in the order: collagen > cPEG > OPF. ICP-OES also showed that the molar Ca:P ratio of collagen and cPEG were similar (1.35 and 1.34, respectively), while that

of OPF was lower (1.27). It should be stressed that ICP-OES is a more accurate method than EDS.

The overall Ca:P ratios as observed using both ICP-OES and EDS may be lower than that of stoichiometric hydroxyapatite (1.67) due to the fact that the source of calcium and phosphate, namely Ca-GP, has a Ca:P ratio of 1. The aforementioned studies reporting hydroxyapatite formation [9, 12, 16, 38] were conducted using mineralization media with Ca:glycerophosphate ratios higher than 1. Moreover, calcium-deficient hydroxyapatite or additional amorphous calcium phosphate may have been formed that are characterized by lower Ca/P ratios.

Small traces of Ca and P were reliably detected by ICP-OES in ALP-free OPF samples (Table 1), in agreement with EDS (Figure 6e)., which is most likely caused by the complexation of calcium to moieties of high affinity for calcium in OPF such as residual carboxylic groups from free fumaric acid or unreacted fumaric endgroups or incomplete washing out of Ca-GP. SEM images of gels with and without ALP mineralized for 6 days are shown in Figure 7. Samples containing ALP (Fig. 7b, d, f) displayed a rougher surface morphology than samples without ALP (Figure 7a, c, e). The morphological changes varied for different materials. In mineralized collagen samples (Figure 7d), mineral appeared to be present in the form of globular deposits with diameters ranging from 100–500 nm, which could be individually visualized. In mineralized cPEG (Figure 7b), spherical structures of approximately the same diameter were observed, however these were tightly packed together. In the case of OPF (Figure 7f), the presence of such structures could not be confirmed. All unmineralized gels (Figure 7a, c, e) were considerably smoother and displayed “worm-like” structures. In unmineralized collagen samples (Figure 7c), rod-like structures with the dimensions of collagen fibrils were formed. [42, 43]

Images of cross-sections of surface regions of mineralized OPF (Figure 7h) showed the presence of a dense outer layer of thickness approximately 15 μm, on top of an inner, porous structure. Surface region cross-sections of mineralized cPEG (Figure 7g) suggested the presence of an outer layer of thickness approximately 30 μm and a dense sub-surface region. No cross-sectional image of mineralized collagen could be taken due to its brittleness in the freeze-dried state.

ALP-induced mineral deposits observed by SEM (Figure 7) were homogeneously distributed throughout the hydrogels in the case of cPEG and collagen. These were spherical and had diameters ranging from 100 to 500 nm. These dimensions are similar to those of the ALP-induced deposits seen on collagen [38] and peptide amphiphile gels [12] while 1–4 μm deposits were seen on polyHEMA. [9, 10] The dimensions of deposits in OPF gels could not be elucidated by SEM. However, the surface morphology was homogenous. Images of gel cross-sections suggested the presence of different layers in surface regions, especially for OPF, where a markedly denser outer layer was observed (Figure 7h). One possible explanation is that more mineralization occurred at the surface than in underlying sub-surface regions.

Histological staining

Light microscopy images of gels containing ALP mineralized for 6 days and subjected to von Kossa staining are shown in Figure 8. All gels stained positive for phosphate deposits (black), with the most intensive staining observed for cPEG. Macropores could be observed in collagen samples.

Quantification of dry mass percentage and mineral:polymer ratio and mechanical testing

The dry mass percentages, i.e. the gel weight percentage not consisting of water, of hydrogels mineralized for 6 days are shown in Figure 9a. Dry mass percentage increase due to raising the ALP concentration from 0 to 1.25 mg ml^{-1} gel was highest for cPEG, followed by collagen and then OPF. All gels showed a significantly higher increase in dry mass percentage when ALP concentration was raised from 0 to 1.25 mg ml^{-1} gel. When ALP concentration was increased from 1.25 to 2.5 mg ml^{-1}, all gels except OPF showed a significant increase.

The mineral:polymer ratios at different ALP concentrations are shown in Figure 9b. The highest increase in ratio was observed for collagen, followed by cPEG and then OPF. This is consistent with the results of ICP-OES analysis (Table 1). Ratio increased from 1.25 to 2.5 mg ALP ml^{-1} for cPEG and collagen but not OPF.

Values of the Young's modulus of cPEG and OPF hydrogels subjected to compressive testing are shown in Figure 10. Mineralized and unmineralized collagen hydrogels were too weak to withstand the testing regimen used. cPEG's Young's Modulus was clearly and significantly higher than OPF's at all ALP concentrations. Values were significantly higher for both hydrogels after raising ALP concentration from 0 to 1.25 mg ml^{-1}. Differences between hydrogels containing 1.25 and 2.5 mg ml^{-1} ALP were only significant for OPF.

Mineralization led to increased stiffness (Figure 10), but the increase was not proportional to the increase in dry mass percentage (Figure 9a), which is a measure of mineral formed. For instance, no significant increase in Young's modulus was observed for cPEG, when ALP concentration was raised from 1.25 to 2.5 mg ml^{-1} gel, although a significant increase in dry mass occurred. These results suggest that excessive mineralization was not accompanied by a strong interaction between polymeric and mineral phases in the in situ formed cPEG composite. Conversely, no significant change in dry mass percentage of OPF occurred between 1.25 and 2.5 mg ALP ml^{-1} gel, but a significant rise in Young's modulus was observed.

Values of the storage and loss modulus of hydrogels subjected to rheological testing are shown in Figure 11. Storage moduli of cPEG samples containing 2.5 mg ml^{-1} ALP were higher by factors of approximately 5 and 8 after 2 and 6 days' mineralization, respectively, compared to samples without ALP (Figure 11a). In the case of OPF, these increases were five- and fifteen-fold, respectively (Figure 11c). In contrast, ALP did not increase the storage modulus of collagen samples after 2 days, and after 6 days, whereas the storage modulus of ALP-containing samples was twice that of ALP-free samples, the loss modulus was approximately three times higher than the storage modulus (Figure 11b). This suggested that while mineralized collagen had become stiffer, it had begun to behave more like a viscous paste than an elastic hydrogel. This latter phenomenon was most likely caused by the lower solid content and gel strength of collagen gels that disintegrate more rapidly than the two synthetic gels of higher solid content and physicochemical stability.

The increase in storage modulus of cPEG and OPF samples containing ALP is consistent with the increase in Young's modulus measured by compressive testing (Figure 10). Values of storage modulus decreased in the order cPEG > OPF > collagen, which is also consistent with the compressive testing results.

The mineral:polymer ratio, as a measure of polymer mineral-forming capacity, was highest for collagen (Figure 9b). The mass percentage attributable to Ca and P was also highest for collagen (Table 1), despite the fact that a significant proportion of ALP was released (Figure 2). One possible explanation is that collagen has a higher density of binding sites for

calcium. Urry et al. reported that collagen contains acidic amino acid sequences that can bind to calcium. [44] Diffusion factors may also play a role in promoting mineral formation. The relatively low concentration of collagen (3 mg/ml) could aid diffusion of the ALP substrate Ca-GP into the hydrogel, promoting mineral formation. The low mineral:polymer ratio in OPF is consistent with the difficulty of visualizing mineral deposits in OPF by SEM (Figure 7), obtaining a XRD diffractogram (Figure 4) and detecting the presence of bands specific for CaP by FTIR (Figure 3).

The increase in dry mass, as a measure of amount of mineral formed, was higher for cPEG than OPF (Figure 9a). This may be due to the calcium-binding properties of the catechol groups in cPEG, which have stimulated CaP formation as components of coatings [26] which means that the presence of calcium-binding groups and incorporation of ALP work synergistically to enhance mineralization.

OPF's mineral:polymer ratio does not increase significantly when ALP concentration is raised from 1.25 to 2.5 mg ml^{-1} gel (Figure 9b). One possible explanation could be limited availability of functional groups in OPF which can act as nucleation sites. Another explanation could be that the higher concentration of OPF polymer in hydrogels (200 mg ml^{-1} compared to 50 mg ml^{-1} for cPEG and 3 mg ml^{-1} for collagen) impedes diffusion of Ca-GP into the hydrogel. If extent of mineralization is limited by availability of nucleation sites and/or diffusion, increasing ALP concentration will not lead to increased mineral formation.

Overall discussion

As stated in the introduction, this study aimed to incorporate ALP into three different hydrogels and investigate a) to what extent ALP is retained in the hydrogel and if it induces mineralization; b) the nature and amount of the mineral thus formed; and c) the effect of mineralization on hydrogel morphology and mechanical properties.

The current study reveals that mineralization of hydrogel materials was obtained by incorporation of ALP followed by incubation in a solution containing calcium ions and glycerophosphate as a substrate for ALP, which cleaves off phosphate which is then free to react with calcium to form insoluble CaP within the hydrogel.

ALP-induced mineralization of all hydrogels was demonstrated by positive von Kossa staining (Figure 8) and the formation of mineral-like deposits as revealed by SEM (Figure 7) exclusively in gels containing ALP. ALP-induced formation of CaP was also demonstrated by FTIR (Figure 3) and XRD (Figure 4) at least in collagen and cPEG hydrogels, while SAED (Figure 5) of cPEG and OPF gels yielded diffractograms characteristic for apatite. From Figure 9 it can be observed that the amount of mineral formation was lowest for OPF gels, which most likely explains the absence of diffraction peaks for mineralized OPF even though SAED confirmed the presence of apatite crystals. It should be realized that the amount of material tested using SAED is much smaller compared to XRD that gives a more reliable overall indication of the mineral-forming capacity of gels. EDS (Figure 6) and ICP-OES (Table 1) proved the presence of Ca and P in all three hydrogel types. Indirect evidence for mineralization was also provided by the considerable increase in dry mass percentage (Figure 9), Young's modulus (Figure 10) and storage modulus (Figure 11) caused by ALP incorporation.

The formation of cPEG and OPF hydrogels is initiated by the strong oxidizing agents $NaIO_4$ and APS, respectively, which would be expected to affect ALP activity. Despite the use of these compounds, sufficient ALP activity was retained to induce mineralization of both cPEG and OPF. One possible explanation is that the major part of these oxidizing agents is

consumed during gel formation by reacting with monomers, which are present in much higher concentrations than ALP. Indeed, in cPEG and OPF hydrogels the ALP:monomer ratio was 5% or less. Hence, only a fraction of these oxidizing agents are left over to react with ALP. These results show that the presence of strong oxidizing agents does not preclude ALP-induced mineralization, suggesting feasibility of ALP addition to other hydrogel types formed using oxidizers.

Beertsen and van den Bos demonstrated that covalent crosslinking of ALP to collagen sheets induced their mineralization [13–15], as did Doi et al. [16] The results show that even highly hydrated collagen hydrogels, from which ALP release is observed, (Figure 2), can be mineralized without a crosslinking step.

Considering in vivo application of mineralized hydrogels, two possible approaches can be envisaged. In the first approach, hydrogel in liquid form containing ALP can be injected into a defect site with subsequent in situ gelation and mineralization. In the second approach, hydrogel samples containing ALP can be pre-fabricated and mineralized under controlled conditions in vitro prior to in vivo implantation. The first approach allows injectability to be preserved, with the associated advantages such as exact molding to the defect site and minimally invasive application. The corresponding disadvantage is the lack of control over the mineralization conditions in situ.

From an analytical point of view, the system described in this paper, namely incorporation of ALP in hydrogels with subsequent incubation in Ca-GP solution, may be used as a method to evaluate the mineral-forming capacity of different hydrogels of interest as bone tissue engineering scaffolds. When comparing the mineralizabilities of different gels, it should be borne in mind that ALP has a negative charge at physiological pH [45] and may thus potentially itself serve as a passive nucleation site for CaP formation. However due to lack of data in literature, discussion on this topic remains speculative for the time being.

Conclusion

This work showed the feasibility of inducing CaP formation in different hydrogels and improving hydrogel mechanical properties by incorporation of ALP during hydrogel formation and subsequent incubation in Ca-GP solution without the need for ALP immobilization by crosslinking. Dry mass percentage as a measure of amount of mineral formed decreased in the order: cPEG > collagen > OPF, whereas mineral:polymer ratio as a measure of polymer mineral-forming capacity decreased in the order: collagen > cPEG > OPF.

Acknowledgments

This research was financed by Agentschap NL, the Netherlands, in the framework of the IOP program “Self Healing Materials”, project no. SHM08717 “Self-healing composites for bone substitution”, and by National Institutes of Health (USA) grant R37 DE014193. Timothy Douglas is currently supported financially by a postdoctoral fellowship from the Research Foundation Flanders (FWO, Belgium). The authors thank Vincent Cuijpers, Tadas Sileika, Natasja van Dijk, Stewart Church and Patrick Larkin for technical assistance.

References

1. Leeuwenburgh SC, Jansen JA, Mikos AG. J Biomater Sci Polym Ed. 2007; 18:1547. [PubMed: 17988519]
2. Leeuwenburgh SC, Ana ID, Jansen JA. Acta Biomater. 2010; 6:836. [PubMed: 19751849]
3. LeGeros, RZ. Calcium Phosphates in Oral Biology and Medicine. Karger; Basel: 1991.

4. Ruhe PQ, Boerman OC, Russel FG, Spauwen PH, Mikos AG, Jansen JA. J Control Release. 2005; 106:162. [PubMed: 15972241]
5. Rowlands AS, George PA, Cooper-White JJ. Am J Physiol Cell Physiol. 2008; 295:C1037. [PubMed: 18753317]
6. Evans ND, Minelli C, Gentleman E, LaPointe V, Patankar SN, Kallivretaki M, Chen X, Roberts CJ, Stevens MM. Eur Cell Mater. 2009; 18:1. [PubMed: 19768669]
7. Boyan BD, Lossdorfer S, Wang L, Zhao G, Lohmann CH, Cochran DL, Schwartz Z. Eur Cell Mater. 2003; 6:22. [PubMed: 14577052]
8. Orimo H. J Nippon Med Sch. 2010; 77:4. [PubMed: 20154452]
9. Filmon R, Basle MF, Atmani H, Chappard D. Bone. 2002; 30:152. [PubMed: 11792578]
10. Filmon R, Basle MF, Barbier A, Chappard D. J Biomater Sci Polym Ed. 2000; 11:849. [PubMed: 11211096]
11. Filmon R, Basle MF, Barbier A, Chappard D. Morphologie. 2000; 84:23. [PubMed: 10923337]
12. Spoerke ED, Anthony SG, Stupp SI. Adv Mater. 2009; 21:425–430. [PubMed: 22068437]
13. Beertsen W, van den Bos T. J Clin Invest. 1992; 89:1974. [PubMed: 1602003]
14. van den Bos T, Beertsen W. J Biomed Mater Res. 1994; 28:1295. [PubMed: 7829559]
15. van den Bos T, Oosting J, Everts V, Beertsen W. J Bone Miner Res. 1995; 10:616. [PubMed: 7610933]
16. Doi Y, Horiguchi T, Moriwaki Y, Kitago H, Kajimoto T, Iwayama Y. Journal of Biomedical Materials Research. 1996; 31:43. [PubMed: 8731148]
17. Brubaker CE, Kissler H, Wang LJ, Kaufman DB, Messersmith PB. Biomaterials. 2010; 31:420. [PubMed: 19811819]
18. Bilic G, Brubaker C, Messersmith PB, Mallik AS, Quinn TM, Haller C, Done E, Gucciardo L, Zeisberger SM, Zimmermann R, Deprest J, Zisch AH. Am J Obstet Gynecol. 2010; 202(1):e1. [PubMed: 20096254]
19. Hunt NC, Grover LM. Biotechnol Lett. 2010; 32:733. [PubMed: 20155383]
20. Temenoff JS, Park H, Jabbari E, Sheffield TL, LeBaron RG, Ambrose CG, Mikos AG. J Biomed Mater Res A. 2004; 70:235. [PubMed: 15227668]
21. Shin H, Quinten Ruhe P, Mikos AG, Jansen JA. Biomaterials. 2003; 24:3201. [PubMed: 12763447]
22. Sugino A, Miyazaki T, Ohtsuki C. J Mater Sci Mater Med. 2008; 19:2269. [PubMed: 18058198]
23. Song J, Saiz E, Bertozzi CR. J Am Chem Soc. 2003; 125:1236. [PubMed: 12553825]
24. Nuttelman CR, Benoit DS, Tripodi MC, Anseth KS. Biomaterials. 2006; 27:1377. [PubMed: 16139351]
25. Chirdon WM, O'Brien WJ, Robertson RE. J Biomed Mater Res B Appl Biomater. 2003; 66:532. [PubMed: 12861604]
26. Ryu J, Ku SH, Lee H, Park CB. Adv Funct Mater. 2010; 20:2132–2139.
27. Lee BP, Dalsin JL, Messersmith PB. Biomacromolecules. 2002; 3:1038. [PubMed: 12217051]
28. Jo S, Shin H, Shung AK, Fisher JP, Mikos AG. Macromolecules. 2001; 34:2839.
29. Karamichos D, Brown RA, Mudera V. J Biomed Mater Res A. 2006; 78:407. [PubMed: 16715519]
30. Schouten C, van den Beucken JJ, de Jonge LT, Bronkhorst EM, Meijer GJ, Spauwen PH, Jansen JA. Biomaterials. 2009; 30:6407. [PubMed: 19717187]
31. Holland TA, Tessmar JK, Tabata Y, Mikos AG. J Control Release. 2004; 94:101. [PubMed: 14684275]
32. Bruder SP, Caplan AI. Bone. 1990; 11:133. [PubMed: 2357424]
33. Pfeilschifter J, Bonewald L, Mundy GR. J Bone Miner Res. 1990; 5:49. [PubMed: 2309578]
34. Pleshko N, Boskey A, Mendelsohn R. Biophys J. 1991; 60:786. [PubMed: 1660314]
35. Fukushima K, Matsuura H. Journal of Molecular Structure. 1995; 350:215.
36. Chang MC, Tanaka J. Biomaterials. 2002; 23:4811. [PubMed: 12361620]
37. Jackson M, Choo LP, Watson PH, Halliday WC, Mantsch HH. Biochim Biophys Acta. 1995; 1270:1. [PubMed: 7827129]

38. Yamauchi K, Goda T, Takeuchi N, Einaga H, Tanabe T. Biomaterials. 2004; 25:5481. [PubMed: 15142729]
39. Koutsopoulos S. J Biomed Mater Res. 2002; 62:600–612. [PubMed: 12221709]
40. Mahamid J, Sharir A, Addadi L, Weiner S. Proc Natl Acad Sci U S A. 2008; 105:12748. [PubMed: 18753619]
41. Tsuji T, Onuma K, Yamamoto A, Iijima M, Shiba K. Proc Natl Acad Sci U S A. 2008; 105:16866. [PubMed: 18957547]
42. Douglas T, Heinemann S, Bierbaum S, Scharnweber D, Worch H. Biomacromolecules. 2006; 7:2388. [PubMed: 16903686]
43. Douglas T, Heinemann S, Mietrach C, Hempel U, Bierbaum S, Scharnweber D, Worch H. Biomacromolecules. 2007; 8:1085. [PubMed: 17378603]
44. Urry DW. Proc Natl Acad Sci U S A. 1971; 68:810. [PubMed: 4251554]
45. Latner AL, Parsons M, Skillen AW. Enzymologia. 1971; 40:1. [PubMed: 5544997]

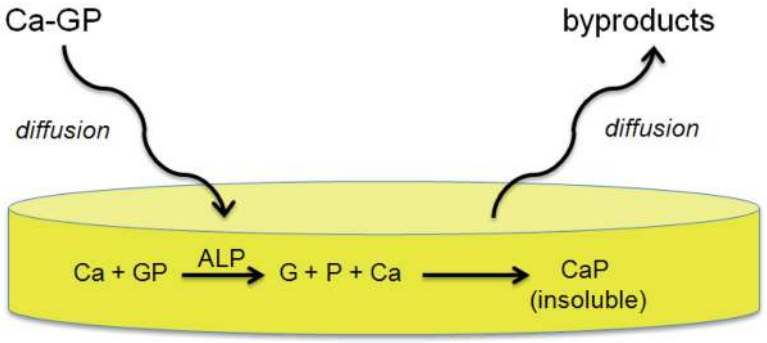

Figure 1.
Basic principle of mineralization by enzymatic action of entrapped Alkaline Phosphatase (ALP). Calcium glycerophosphate (Ca-GP) diffuses into hydrogels with incorporated ALP. Inside the hydrogel, glycerophoshate (GP) is cleaved to phosphate (P) by ALP, which subsequently reacts with Ca^{2+} ions to form insoluble calcium phosphate (CaP) which remains inside the hydrogel.

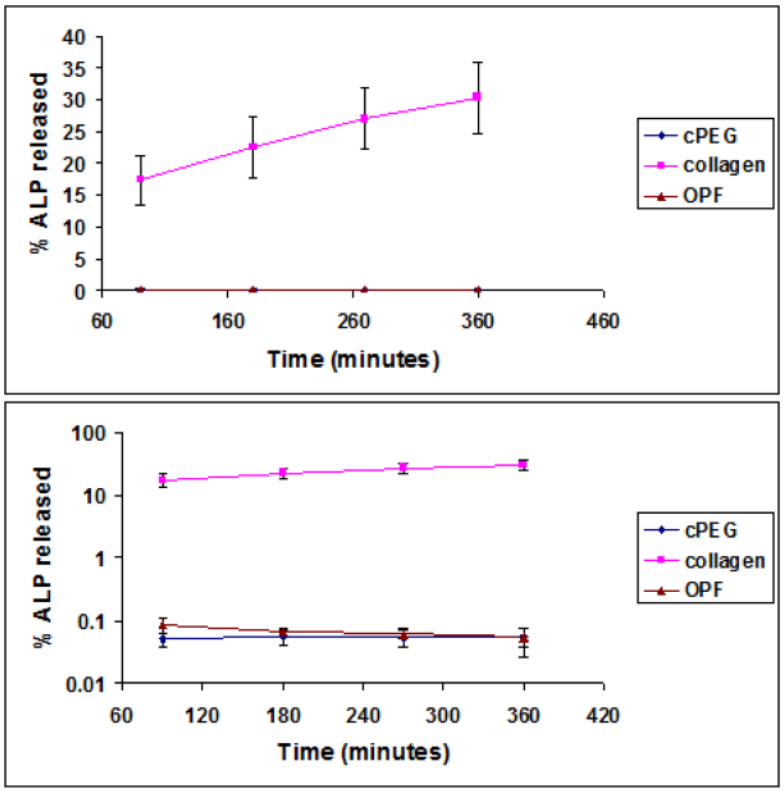

Figure 2.
Release of ALP from hydrogels. Top: with linear y-axis; bottom: logarithmic y-axis. Error bars show standard deviation.

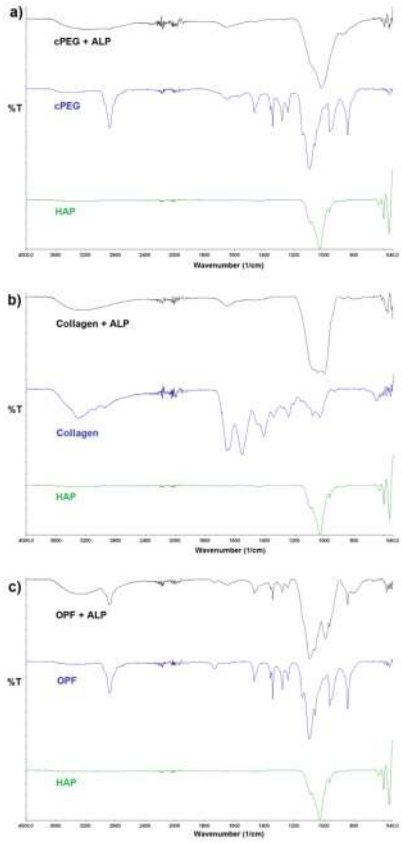

Figure 3.
FTIR spectra of freeze-dried hydrogels with ALP concentrations of 2.5 mg ml^{-1} (top, black) and 0 mg ml^{-1} (middle, blue) mineralized for 6 days. A spectrum of hydroxyapatite (green, bottom) is given as a reference. a: cPEG; b: collagen; c: OPF.

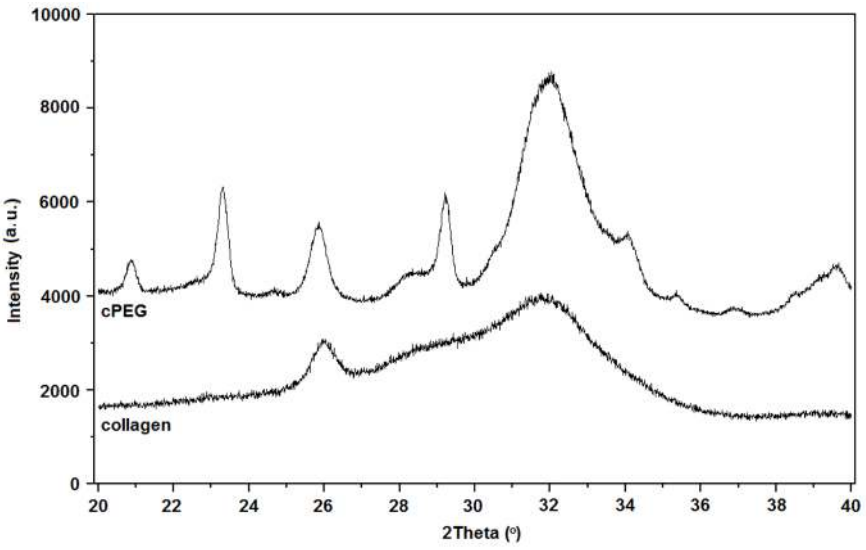

Figure 4.
XRD spectra of freeze-dried cPEG (top) and collagen (bottom) hydrogels with ALP concentrations of 2.5 mg ml^{-1}) mineralized for 6 days.

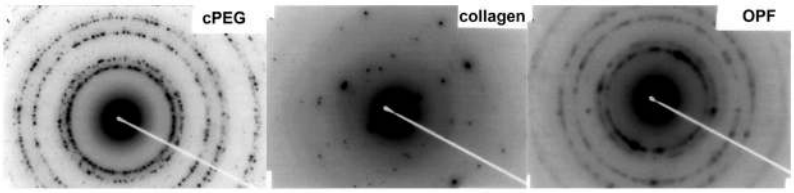

Figure 5.
SAED diffractograms of freeze-dried hydrogels with ALP concentrations of 2.5 mg ml^{-1} mineralized for 6 days. Left: cPEG; middle: collagen; right: OPF.

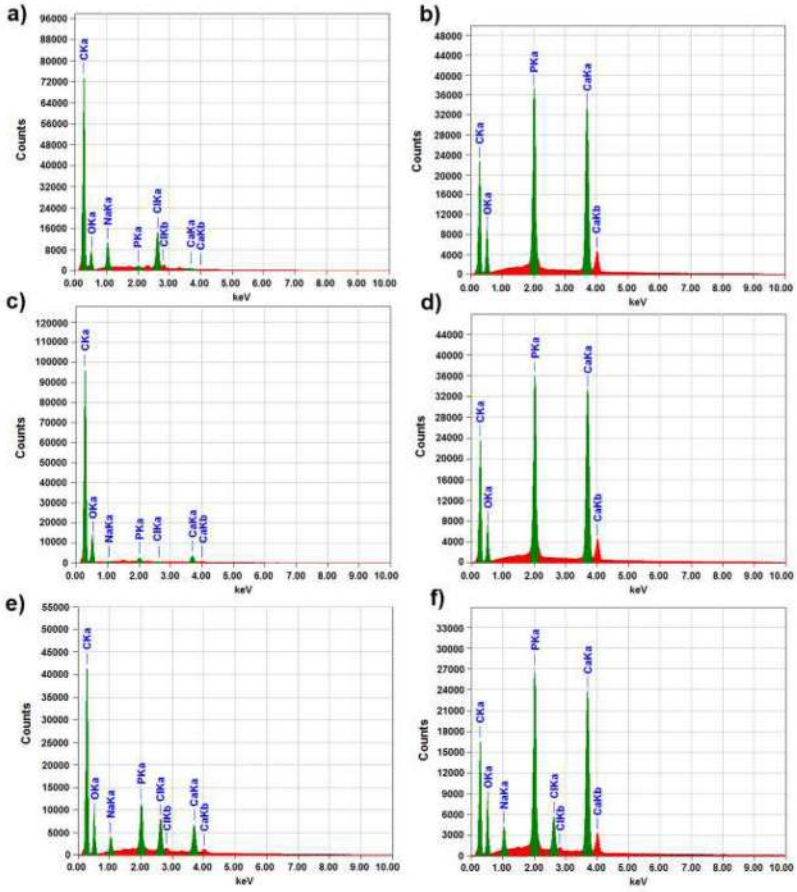

Figure 6.

EDS spectra of freeze-dried hydrogels containing ALP at concentrations of 0 (a, c, e) and 2.5 (b, d, f) mg ml^{-1} mineralized for 6 days. a, b: cPEG; c, d: collagen; e, f: OPF. Ka, Kb denote K-alpha and beta emissions, respectively.

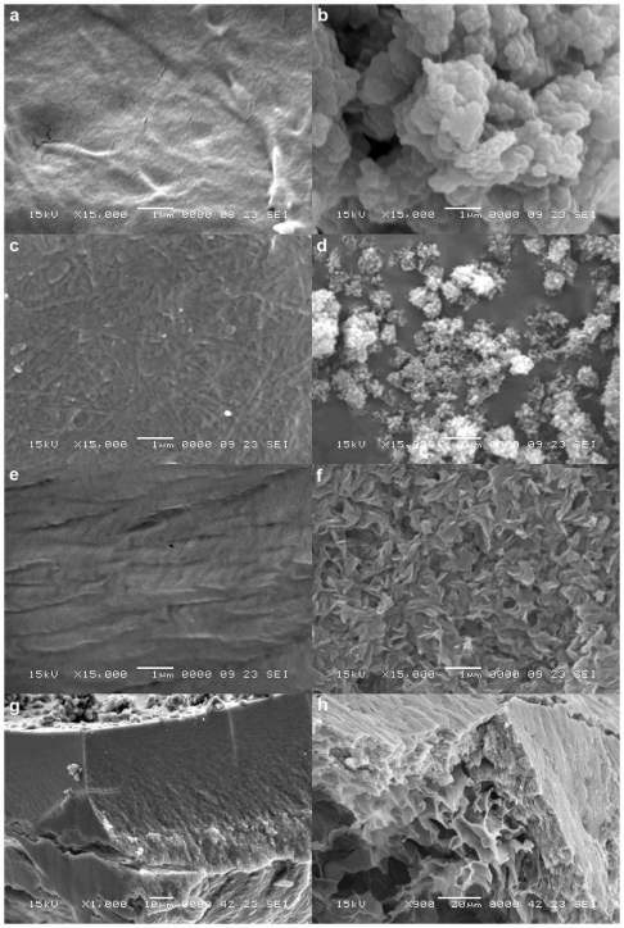

Figure 7.
SEM Images of freeze-dried hydrogels containing ALP at concentrations of 0 (a, c, e) and 2.5 (b, d, f) mg ml^{-1} mineralized for 6 days. a, b: cPEG; c, d: collagen; e, f: OPF. Cross-sectional images of cPEG (g) and OPF (h) containing 2.5 mg ml^{-1} ALP are also shown.

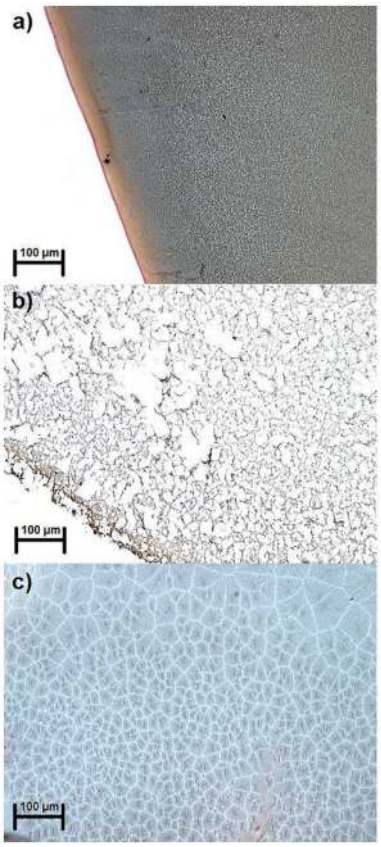

Figure 8.
Von Kossa staining for phosphate deposits. Light microscopy images of stained cross-sections of gels containing ALP (a: cPEG; b: collagen; c: OPF) at a concentration of 2.5 mg ml^{-1} mineralized for 6 days. Black staining is characteristic for phosphate deposits.

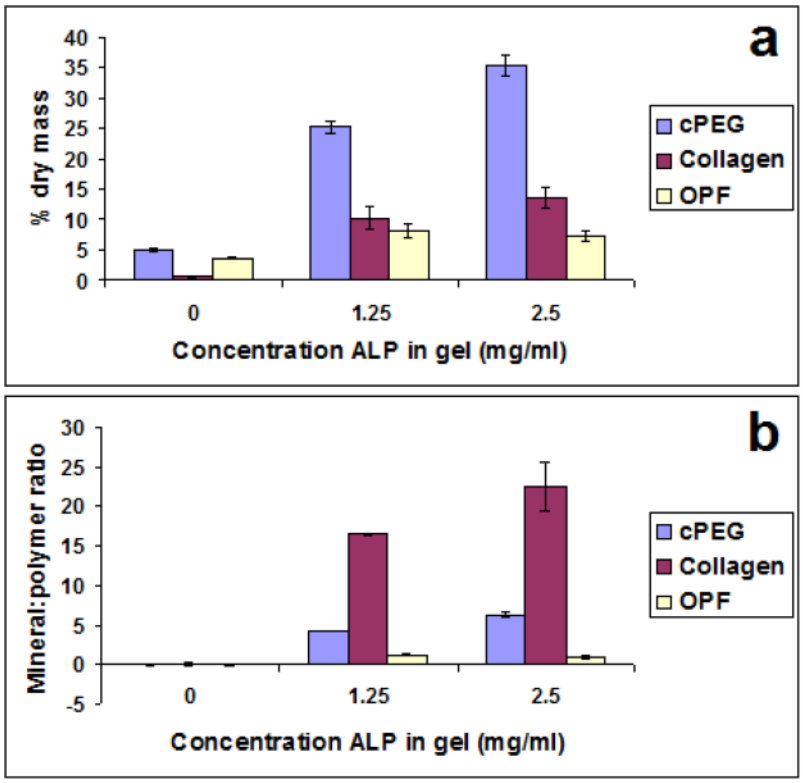

Figure 9.

a) Dry mass percentages of hydrogels with ALP concentrations of 0, 1.25 and 2.5 mg ml^{-1} mineralized for 6 days. Error bars show standard deviation. Significant differences ($p < 0.01$ in all cases): between 0 and 1.25 mg ml^{-1} for all hydrogels, between 1.25 and 2.5 mg ml^{-1} for cPEG and collagen. b) Mineral:polymer ratio in hydrogels at ALP concentrations of 0, 1.25 and 2.5 mg ml^{-1} after 6 days' mineralization. Error bars show standard deviation.

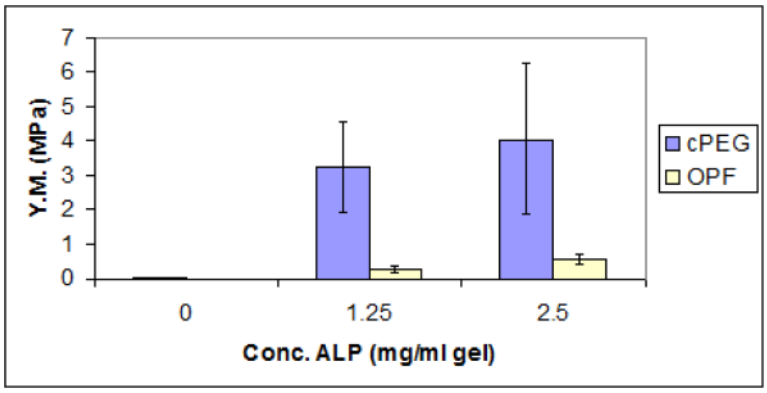

Figure 10.

Young's modulus (Y. M.) of cPEG and OPF gels subjected to compressive testing after 6 days of enzymatic mineralization. Error bars show standard deviation. Significant differences ($p < 0.01$ in all cases): between cPEG and OPF at all ALP concentrations, between 0 and 1.25 mg ALP ml^{-1} gel for cPEG and OPF, between 1.25 and 2.5 mg ALP ml^{-1} gel for OPF only.

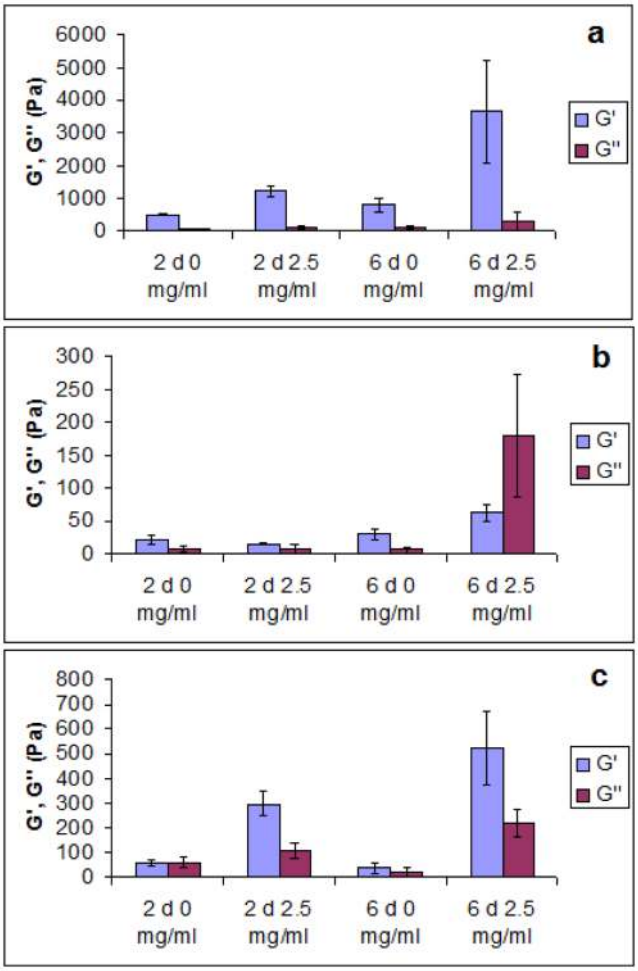

Figure 11.

Measurement of storage modulus (G′) and loss modulus (G″) of cPEG (a), collagen (b) and OPF (c) hydrogels containing 0 and 2.5 mg ALP/ml gel after 2 and 6 days of enzymatic mineralization. Error bars show standard deviation. Significant differences: between 2 d 0 mg ml^{-1} and 2 d 2.5 mg ml^{-1}: cPEG and OPF; between 6 d 0 mg ml^{-1} and 6 d 2.5 mg ml^{-1}: all three materials; between 2 d 2.5 mg ml^{-1} and 6 d 2.5 mg ml^{-1}: collagen only.

Table 1

ICP-OES determination of Ca and P mass percentages and molar Ca:P ratio in lyophilized hydrogel samples

Hydrogel material	Conc. ALP [mg/mg hydrogel]	Mass percentage Ca [%]	Mass percentage P [%]	Molar Ca:P ratio [–]
cPEG	0	< 1.3 *a)*	< 0.3 *a)*	-
cPEG	2.5	24.7	14.3	1.34
Collagen	0	< 2.0 *a)*	< 1.0 *a)*	-
Collagen	2.5	29.0	16.6	1.35
OPF	0	4.1	1.7	-
OPF	2.5	15.0	9.2	1.27

a) Raw data signal was below accurate detection limit of instrumentation.